RSC Advances

Bulk and solution properties of thermo-responsive rod-coil block polymer based on poly(N-isopropylacrylamide)

Journal:	*RSC Advances*
Manuscript ID:	RA-ART-07-2014-007179.R1
Article Type:	Paper
Date Submitted by the Author:	16-Sep-2014
Complete List of Authors:	Liu, Peng; Institute of Polymer Science, College of Chemistry Liang, Jiexing; Institute of Polymer Science, College of Chemistry chen, sheng; Institute of Polymer Science, College of Chemistry zhang, hailiang; Institute of Polymer Science, College of Chemistry

Table of contents entry：

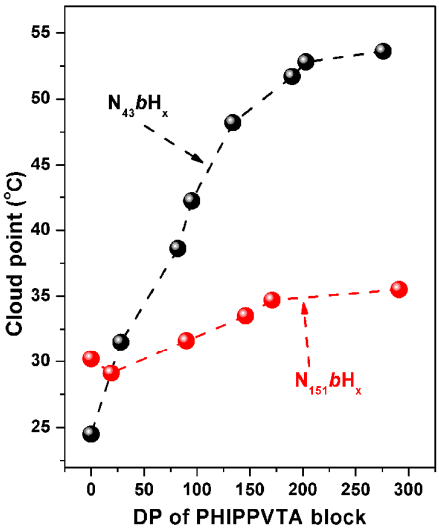

Highlight

- Molecular weight dependence on thermoresponsive behaviors of rod-coil diblock copolymers (x indicates the DP of rod PHIPPVTA blocks).

Cite this: DOI: 10.1039/c0xx00000x

www.rsc.org/xxxxxx

PAPER

Bulk and solution properties of thermo-responsive rod-coil block polymer based on poly(*N*-isopropylacrylamide)

Peng Liu[a,b], Jiexing Liang[a], Shen Chen[a] and Hailiang Zhang*[a]

Received (in XXX, XXX) Xth XXXXXXXXX 20XX, Accepted Xth XXXXXXXXX 20XX

DOI: 10.1039/b000000x

A series of thermo-responsive rod-coil diblock copolymers with well-defined molecular weights have been synthesized via reversible addition-fragmentation chain transfer (RAFT) polymerization. The rod-coil diblock thermo-responsive copolymer studied herein is poly(*N*-isopropylacrylamide)-*b*- poly[bis(*N*-hydroxyisopropyl pyrrolidone) 2-vinylterephthalate] (PNIPAm-*b*-PHIPPVTA), in which PHIPPVTA is a thermo-responsive rod-like polymer and exhibits an MW-dependent liquid crystalline (LC) phase behavior and MW-dependent thermo-responsive behavior. The bulk phase behaviors of the copolymers have been investigated by a combination of techniques including differential scanning calorimetry (DSC), polarized light microscopy (PLM), 1D and 2D wide-angle X-ray diffraction. The experiment results demonstrated phase structure of PNIPAm-*b*-PHIPPVTA is a hexatic columnar nematic phase when $N_{43}bH_x$ and $N_{151}bH_x$ with $X \geq 95$ and 146, respectively. The thermo-responsive behaviors were investigated with turbidity measurements using UV-visible spectroscopy. The results showed that the cloud point of the diblock copolymers PNIPAm-*b*-PHIPPVTA can be adjusted by varying the length of the PHIPPVTA block. Only one phase transition temperature has been observed in the thermo-responsive rod-coil diblock copolymer PNIPAm-*b*-PHIPPVTA. Of special interest is the cloud point of block copolymers with longer flexible chain segment more strongly depending on the length of the semirigid segment compared to copolymers with shorter flexible chain segment.

Introduction

Thermo-responsive block copolymers have attracted ever-increasing attention in the past decades due to their promising applications as drug delivery systems,[1,2] smart wound dressings,[3] industrial applications,[4,5] smart gels and tissue engineering.[6-8] Some water-soluble block copolymers usually dissolve when cooled and separate from the aqueous solution when heated above the critical temperature. This critical temperature is called lower critical solution temperature (LCST). Conventionally, the phase transitions are generally induced by imbalance and competition between polymer-polymer interactions and the hydration of polymer. It was shown that the LCST can be adjusted by altering the hydrophilic-hydrophobic property of block copolymers. In addition, the LCST of the block polymer can be also tuned to a desired temperature range by external stimuli such as pH, salt and light, etc.[9-18] The most extensively investigated thermo-responsive block copolymers consist of poly(*N*-isopropylacrylamide) (PNIPAm) block. PNIPAm undergoes a sharp coil-to-globule transition in water closer to the human body temperature (32 °C), changing from a hydrophilic state below this temperature to a hydrophobic state above it.[19-21] By incorporating a hydrophilic comonomer like poly(ethylene oxide) (PEO) or polyacrylic acid (PAA),[22-25] it is possible to shift the LCST to higher temperatures. On the contrary, by incorporating a hydrophobic comonomer like polystyrene (PS) or poly(tert-butyl methacrylate), it is possible to shift the LCST to lower temperatures.[26,27]

Moreover, several interesting studies have been reported, thermo-responsive block copolymers were also synthesized to consist of two thermo-responsive blocks. For example, poly(*N*-isopropylacrylamide)-*block*-poly(3-[*N*-(3-methacryl amido propyl)-*N*, *N*-dimethyl] ammoniopropane sulfonate) with double thermo-response was synthesized, using two blocks that possessed both LCST and upper critical solution temperature (UCST).[28] Zhao et al. synthesized very interesting block copolymer, poly(methoxytri (ethylene glycol) acrylate-*co*-acrylic acid)-*block*-poly(ethoxydi(ethylene glycol) acrylate-co-acrylic acid) with C-shaped sol-gel phase diagram. A 20 wt% aqueous solution of the diblock copolymer with pH of 3.29 underwent sol-to-gel, gel-to-sol, and clear sol-to-cloudy sol transitions at 17 °C ($T_{sol-gel}$), 38 °C ($T_{gel-sol}$), and 55 °C ($T_{clouding}$), respectively, upon heating.[29] Laschewsky et al. synthesized the novel block

[a] *Key laboratory of polymeric materials & application technology of Hunan Province, key laboratory of advanced functional polymer materials of colleges of Hunan Province, College of Chemistry, Xiangtan University, Xiangtan, Hunan, 411105, China. Email: zhl1965@xtu.edu.cn*

[b] *College of Chemisty and Chemical Engineering, Qujing Normal University, Qujing, Yunnan, 655011, China. Email: liupengxj@gmail.com*

copolymer poly[4-vinylbenzyl methoxytetrakis(oxyethylene) ether]-*block*-poly[4-vinylbenzyl methoxytetrakis (oxyethylene) ether-*alt*-*N*-methylmaleimide].[30] Each block shows the LCSTs at about 28 and 39 °C, respectively. They studied the thermally induced associate formation in water by turbidity and dynamic light scattering measurement.

The linearly thermo-responsive block copolymers have gained much impetus in recent years due to the enhance boost of the so-called controlled free radical polymerization methods, such as nitroxyl-mediated free radical polymerisation, atom transfer free radical polymerization (ATRP),[31-33] or reversible addition fragmentation chain transfer (RAFT) polymerization.[34-38] RAFT polymerization is often a method of choice when control on molecular weight and molar mass distribution is needed. RAFT mediated by thiocarbonyl compounds is an effective and versatile process, applicable to a wide range of vinyl monomers without a need for protecting group.

These extensively investigated linear thermo-responsive block copolymers are coil-coil block copolymer. A few thermo-responsive rod-coil block copolymers consisting of rigid chain such as oligo(para-phenylene) or hydrophilic maltoheptaose have been synthesized and studied.[39,40] There is lack of thermosensitivity in the rigid segment of these thermo-responsive rigid-flexible block copolymers. Some thermo-responsive natural polymers (i.e., polypeptide or polysaccharides) are used as rod segment in thermo-responsive rod-coil block copolymers.[41,42] Yet it is difficult to tune their properties by changing their molecular weights, which limited their applications. The novel semirigid water-soluble thermo-responsive polymers based on mesogen-jacketed liquid crystal polymers have been the subject of intense study in recent years.[43-45] Unusual solution phase transition trend of the semirigid water-soluble polymers were explored for the first time by our group.[44-46] The molecular structure and molecular weight of this semirigid water-soluble thermo-responsive polymers based on mesogen-jacketed liquid crystal polymers easy to control. Encouraged by those results, we designed and synthesized a series of semirigid-flexible block copolymers based on semi-rigid polymer (i.e., poly[bis(*N*-hydroxyisopropyl pyrrolidone) 2-vinylterephthalate]) and flexible chain polymer (i.e., PNIPAm) via reversible addition-fragmentation chain transfer (RAFT). And we expect the thermo-responsive behaviors of diblock copolymers to be strongly dependent upon the lengths of semirigid block HIPPVTA units similar to the cases of homopolymer PHIPPVTA.

In this account, we have employed semirigid-flexible block copolymers consisting of poly[bis(N-hydroxyisopropyl pyrrolidone) 2-vinylterephthalate] (PHIPPVTA) rod units as a semirigid segment, and flexible chains such as PNIPAm for the construction of various self-assembled structures in bulk and aqueous solution. These linear rod-coil diblock copolymers with various amounts of HIPPVTA comonomer enable to modulate the phase transition temperature. To the best of our knowledge, this is the first study on tunable thermo-responsive behaviors of the semirigid-flexible block copolymers by adjusting length of thermo-responsive segment. Additionally, the linear rod-coil block copolymers prepared here with various combinations of semirigid segment (PHIPPVTA block) were found to be liquid-crystalline behavior by choosing appropriate degree of polymerization (DP) of semi-rigid PHIPPVTA block.

Experimental

Materials

N,*N*-dimethylformamide (DMF) and trichloromethane were purchased from Shanghai Chemical Reagents Co., A.R. grade and purified by drying over anhydrous magnesium sulfate and distilled. Acetone (Beijing Chemical) was refluxed over potassium permanganate and distilled before use. 4-Dimethylaminopyridine (DMAP) was purchased from Haili Chemical Reagents Co. and purified by recrystallization twice from benzene. 1-Amino-2-propanol and γ-butyrolactone were purchased from Shanghai Chemical Reagents Co., A.R. grade. Azobisisobutyronitrile (AIBN) was purchased from Shanghai Chemical Reagent Company and purified by recrystallization twice from ethanol. Tri-n-butyltin hydride (97%) was purchased from Aladdin. Deionized (DI) water was obtained from a reagent water system (Aquapro) with a specific resistivity of 18.25 MΩ cm^{-1}. All the other chemicals were used as received. 2-(Ethylsulfanylthiocarbonylsulfonyl)-2-methylpropionic acid (EMP), 2-Vinyl p-biphthalic acids (VTA) and 2-vinylterephthaloyl chloride were synthesized according to reported methods.[47,43,48,49]

Polymerization procedures

Synthesis of Macromolecular Chain Transfer Agent (macro-CTA). Polymerizations were conducted at 75 °C, employing AIBN as the primary radical source and 2-ethylsulfanylthiocarbonylsulfonyl-2-methylpropionic acid (EMP) as the RAFT chain transfer agent (CTA). The synthetic route is shown in Scheme 1. A typical polymerization procedure is as follows: NIPAm (1.0 g, 8.85×10^{-3} mol), EMP (3.96×10^{-2} g, 1.77×10^{-4} mol) and AIBN (2.32×10^{-3} g, 1.41×10^{-5} mol) were added to a reaction tube, followed by the addition of 1.5 ml of DMF. After three freeze-pump-thaw cycles, the tube was sealed under vacuum. The polymerization was carried out at 75 °C for 4.5 h and stopped by exposing to air. The polymerization solution was diluted with dichloromethane, followed by slowly precipitating from large amount of petroleum ether. The product (macro-CTA) was further purified by re-dissolving in dichloromethane and precipitated from petroleum ether three times. Finally, a straw yellow solid product was obtained after drying under vacuum at 50 °C (0.86 g, yield = 86.0%). The macro-CTAs were named as N_{43} and N_{151} (subscript indicates the number of the NIPAm unit, Table 1).

Synthesis of Semirigid-flexible Block Copolymer PNIPAm-b-PHIPPVTA by RAFT Polymerization. The monomer bis(*N*-hydroxyisopropyl pyrrolidone) 2-vinylterephthalate (HIPPVTA) was synthesized according to reported methods in our previous work.[44] The PNIPAm-*b*-PHIPPVTA was prepared by the similar process as macro-CTA. Typically, 0.22g of HIPPVTA (5.14×10^{-4} mol) and 0.1g of macro-CTA1 (2.05×10^{-5} mol) were dissolved in 80 mL of DMF containing 3.02×10^{-5} g of AIBN (1.84×10^{-6} mol) in a reaction tube. After three freeze-pump-thaw cycles, the tube was sealed under vacuum. The polymerization was carried out at 75 °C for 4.5 h and stopped by exposing to air. Then, the reaction mixtures were poured into ether to precipitate the resulting PNIPAm-*b*-PHIPPVTA copolymers. The resulting

polymer was collected by filtration and purified twice by redissolution/reprecipitation with THF/ether, and finally dried in vacuum overnight. A straw yellow solid product was obtained (0.28 g, yield = 87.5%). The synthetic route is shown in Scheme 1. The resultant copolymers were named as $N_{43}bH_x$ and $N_{151}bH_x$ (subscript x indicates the number of the HIPPVTA unit, Table 1).

Characterizations

^1H NMR. ^{1}H NMR spectra were recorded on a BRUKER ARX400 MHz spectrometer with tetramethylsilane (TMS) as the internal standard at room temperature in $CDCl_3$. Chemical shifts (δ) were given in ppm relevant to TMS.

Gel Permeation Chromatography (GPC). GPC measurements were performed on a PL-GPC120 setup equipped with a column set consisting of two PL gel 5 μm MIXED-D columns (7.5 × 300 mm, effective molecular weight range of 0.2 ~ 400.0 kg mol^{-1}) using DMF that contained 0.01 M LiBr as the eluent at 80 °C at a flow rate of 1.0 ml min^{-1}. Narrowly distributed polystyrene standards in the molecular weight range of 0.5 ~ 7.5 × 10^7 g mol^{-1} (PSS, Mainz, Germany) were utilized for calibration.

Differential Scanning Calorimetry (DSC). DSC examination was carried out on a TA DSC Q100 calorimeter with a programmed heating procedure in nitrogen. The sample size was about 5 mg and encapsulated in hermetically sealed aluminum pans, whose weights were kept constant. The temperature and heat flow were calibrated using standard materials (indium and zinc) at the cooling rate (10 ^{o}C min^{-1}) and the heating rate (20 ^{o}C min^{-1}). The temperature and heat flow scale at different cooling and heating rates were calibrated, using standard materials such as indium and benzoic acid.

Polarized Light Microscope (PLM). Liquid-crystalline (LC) texture of the polymers was observed under PLM (Leica DM-LM-P) coupled with a Mettler-Toledo hot stage (FP82HT). The films with thickness of ~ 10 μm were casted from CH_2Cl_2 solution and slowly dried at room temperature.

One-dimensional Wide-angle X-ray Diffraction (1D WAXD). The supermolecular structures of PHIPPVTA polymers were examined by 1D WAXD thermal experiments. 1D WAXD powder experiments were performed on a Bruker AXS D8 Advance diffractometer with a 40 kV FL tubes as the X-ray source (Cu Kα) and the LYNXEYE_XE detector. The reflection peak positions were calibrated with silicon powder (2θ > 15°) and silver behenate (2θ < 10°). The sample stage was set horizontally, and a temperature control unit (Anton Paar TCU 110) in conjunction with the diffractometer was utilized to study the structure evolutions as a function of temperature. The heating and cooling rates in the WAXD experiments were 5 ^{o}C min^{-1}. The sample temperature was controlled within ± 1 ^{o}C. The background scattering was recorded and subtracted from the sample patterns.

Two-dimensional Wide-angle X-ray Diffraction (2-DWAXD). 2D WAXD was carried out using a Bruker AXS D8 Discover diffractometer with a 40 kV FL tubes as the X-ray source (Cu Kα) and the VANTEC 500 detector. The oriented samples were prepared by mechanically shearing from the LC phase when applicable. The point-focused X-ray beam was aligned either perpendicular or parallel to the mechanical shearing direction. The background scattering was recorded and subtracted from the sample patterns.

Turbidity Measurement. The aggregation behavior of the polymer solutions was measured in a UV−Vis spectrophotometer (PerkinElmer Lambda 25). The aqueous solution of block copolymer was prepared by dissolving the polymer powder in water followed by overnight refrigeration to ensure complete dissolution, then diluting with deionized water to obtain the desired concentration. The transmittance of the block copolymer solutions were monitored in a 1 cm quartz sample cell as a function of temperature at a wavelength of 500 nm. Heating and cooling scans were performed between 20 and 80 °C at a scanning rate of 1.0 °C min^{-1} with hold steps of 10 min at each temperature. The phase separation temperatures (cloud point) of the polymer solutions were determined at 50% transmittance.

Dynamic Light Scattering (DLS). DLS measurements were conducted on a commercial spectrometer (BI-200 SM) equipped with a multitau digital time correlator (BI-9000) and an adjustable solid-state laser emitting (output power of ~ 40 mW at a wavelength of λ = 532 nm) as the light source. A temperature controller (BI-TCD) was utilized for precisely adjusting the solution temperature. The solutions were heated in steps and stabilized for 10 min before the data were recorded. All the DLS measurements were done at an angle of 90^o, The CONTIN Laplace inversion algorithm in the correlator was used, and the intensities of light scattering were recorded.

Results and discussion

Synthesis and bulk property of the block copolymer PNIPAm-*b*-PHIPPVTA

In this work, two series of PNIPAm-*b*-PHIPPVTA block copolymers with different molecular weights were synthesized through RAFT polymerization. The macro-CTAs (N_{43} and N_{151}) were synthesized through the RAFT polymerization using EMP as a CTA. GPC analysis was performed to determine the macro-CTA molecular weight (MW) and polydispersity index (PDI). The macro-CTAs (N_{43} and N_{151}) show monodispersed distributions and various GPC traces, indicating various MWs and approximate PDIs of N_{43} (M_n = 0.57 × 10^4, *PDI* = 1.04) and N_{151} (M_n = 1.99 × 10^4, *PDI* = 1.03). The monomer of the PHIPPVTA block, HIPPVTA, was prepared and characterized as described in our previous work.[44] Using trithiocarbonate-terminated PNIPAm (N_{43} and N_{151}) as macro-CTA, AIBN as initiator, and DMF as solvent, a variety of PNIPAm-*b*-PHIPPVTA diblock copolymers were synthesized by changing the ratio of macro-CTA to monomer. The detailed synthesis route is illustrated in Scheme 1.

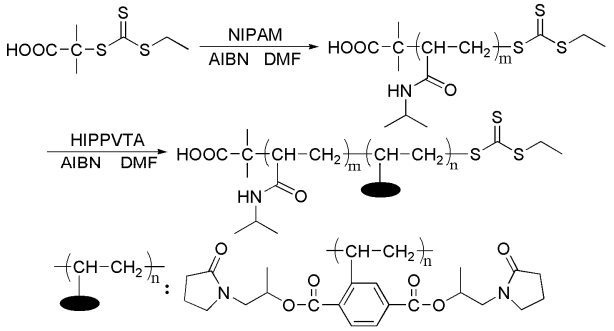

Scheme 1 Synthetic route of PNIPAm-*b*-PHIPPVTA diblock copolymers

The chemical structures of the PNIPAM macro-CTA and PNIPAm-*b*-PHIPPVTA diblock copolymer were characterized by ^{1}H NMR spectroscopy (Fig.1). For macro-CTA PNIPAM, the peaks at 3.31 ppm (peak p) and 4.0 ppm (peak b) are attributed to the resonance of methylene protons of ethylsulfanylthiocarbonyl group and methine proton of isopropyl group, respectively. The ratio of integration intensity of the resonance at 3.31 ppm to that of the resonance at 4.0 ppm was measured to be about 2:43 for the N_{43} and 2:151 for the N_{151}. According to the ratio of integration intensity, the molecular weight of PNIPAM N_{43} and N_{151} were calculated to be $M_n = 4.86 \times 10^3$ g mol^{-1} and $M_n = 1.71 \times 10^4$ g mol^{-1}, respectively (Table 1). The molecular weight (M_n) and molecular weight distribution (M_w/M_n) of the linear block copolymers were characterized by GPC. The chain length and the composition of the block copolymers were calculated by ^{1}H NMR data. For example, $PNIPAm_{43}$, $PNIPAm_{43}$-*b*-$PHIPPVTA_{28}$, $PNIPAm_{43}$-*b*-$PHIPPVTA_{75}$, $PNIPAm_{43}$-*b*-$PHIPPVTA_{134}$, $PNIPAAm_{43}$-*b*-$PHIPPVTA_{203}$ and $PNIPAm_{43}$-*b*-$PHIPPVTA_{276}$ were synthesized (each subscript indicates the number of the monomer unit), and these polymers were abbreviated as N_{43}, $N_{43}bH_{28}$, $N_{43}bH_{75}$, $N_{43}bH_{134}$, $N_{43}bH_{203}$ and $N_{43}bH_{276}$, respectively. These linear polymers consisted of PHIPPVTA content ($f_{PHIPPVTA}$) of 0, 39.44, 63.56, 68.84, 75.71 and 86.52 mol% in the block copolymers, respectively. According to the previous literatures, the density of the flexible chain PNIPAm was 1.07 g cm^{-3} at room temperature.[50,51] The density of PHIPPVTA was determined to be 1.25 g cm^{-3} by suspension method. Combining the data of density and $f_{PHIPPVTA}$, we can further estimate the volume fraction of PHIPPVTA ($V_{PHIPPVTA}$) according to reported methods.[52] The rod-coil diblock copolymers possess the $V_{PHIPPVTA}$ values ranged from 29.56% to 95.48%. All sample information such as molecular weights, polydispersity, thermal properties, mol fraction and volume fraction can be found in Table 1.

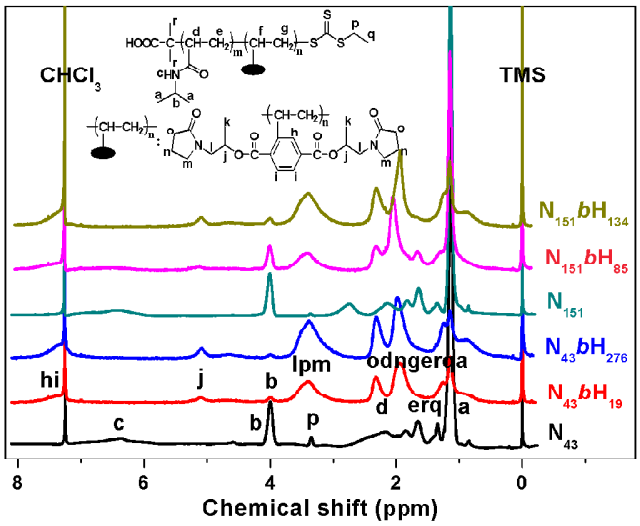

Fig.1 ^{1}H NMR spectra of macro-CTA PNIPAm and PNIPAm-*b*-PHIPPVTA diblock copolymers in $CDCl_3$.

Table 1 Molecular characteristics and properties of P(NIPAm-*b*-HIPPVTA)

Sample [a]	Mn ($\times 10^4$) [b]	PDI [b]	Mn ($\times 10^4$) [c]	PHIPPVTA Content [d]	$V_{PHIPPVTA}$ [e]	T_g (°C) [f]	T_d (°C) [g]	CP (°C) [h]	LC [l]
N_{43}	0.57	1.04	0.48	0%	0%	114.9	249.8	24.5	N
$N_{43}bH_{28}$	1.46	1.21	1.72	39.44%	68.57%	95.6	265.8	31.5	N
$N_{43}bH_{75}$	1.94	1.19	4.24	63.56%	86.71%	93.8	301.8	38.6	N
$N_{43}bH_{95}$	2.76	1.24	4.68	68.84%	87.95%	90.1	304.9	42.5	Y
$N_{43}bH_{134}$	3.49	1.28	6.41	75.71%	91.19%	87.0	309.6	48.2	Y
$N_{43}bH_{190}$	4.46	1.29	8.88	81.55%	93.61%	87.1	316.4	51.7	Y
$N_{43}bH_{203}$	5.21	1.32	9.46	82.53%	93.98%	85.7	323.5	52.8	Y
$N_{43}bH_{276}$	6.58	1.38	12.68	86.52%	95.48%	85.6	321.9	53.6	Y
N_{151}	1.99	1.03	1.71	0%	0%	134.4	346.3	30.2	N
$N_{151}bH_{19}$	2.42	1.12	2.55	11.18%	29.56%	112.2	308.9	29.1	N
$N_{151}bH_{90}$	3.28	1.18	5.68	37.34%	66.52%	105.5	321.5	31.6	N
$N_{151}bH_{146}$	4.48	1.27	8.16	49.16%	76.31%	104.6	321.1	33.5	Y
$N_{151}bH_{171}$	5.32	1.33	9.26	53.11%	79.05%	90.2	315.9	34.7	Y
$N_{151}bH_{291}$	6.65	1.39	14.57	65.84%	86.55%	88.5	315.7	35.5	Y

[a] *N_{43} and N_{151} were showed the polyNIPAm$_{43}$ and polyNIPAm$_{151}$, respectively. N_xbH_y were showed the polyNIPAm$_x$-b-polyHIPPVTA$_y$.*

[b] *The Mn and PDI of copolymers were measured by GPC using PS standards and DMF as solvent.*

[c] *Calculated Mn by ^{1}H NMR.*

[d] *Calculated PHIPPVTA content of the block copolymer (mol%) by ^{1}H NMR.*

[e] *Estimated based on Ref. 49.*

[f] *The Tg was obtained by DSC at a heating rate of 10 °C min^{-1} under N_2 during the second heating process.*

[g] *The decomposition temperatures at 5% weight loss of the samples measured by TGA heating experiments at a rate of 20 °C min^{-1} under N_2.*

[h] *The copolymers were dissolved in the highly pure deionized water and then the cloud point (CP) of aqueous polymer solutions (10.0 mg ml^{-1}) were measured by turbidimetry.*

[l] *LC was observed by polarized optical microscopy..*

The degree of polymerization (DP) of block polymers by both methods was confirmed by means of ^{1}H NMR and elemental analysis. The results of ^{1}H NMR and elemental analysis of the polymers are listed in Table 1 and Table S1, respectively. Some deviation in carbon analysis noticed between the calculated and experimental values for the proposed structures in Table S1. This

possibly was caused by the hygroscopic nature of hydrophilic group of these polymers.[53,54] But the experimental values coincide essentially with calculated values by ^{1}H NMR. For instance, Anal. Calcd for N_{43} ($C_{265}H_{485}N_{43}O_{45}S_3$): C, 62.53; H, 9.60; N, 11.83; S, 1.89; Found: C, 62.07; H, 9.69; N, 11.56; S, 1.84. Anal. Calcd for $N_{43}bH_{28}$ ($C_{937}H_{1325}N_{99}O_{213}S_3$): C, 64.38; H, 7.64; N, 7.93; S, .55; Found: C, 63.22; H, 7.91; N, 7.76; S, 0.51. Anal. Calcd for N_{151} ($C_{913}H_{1673}N_{151}O_{153}S_3$): C, 63.35; H, 9.74; N, 12.22; S, 0.56; Found: C, 61.89; H, 9.87; N, 12.06; S, 0.52. Anal. Calcd for $N_{151}H_{19}$ ($C_{1369}H_{2243}N_{189}O_{267}S_3$): C, 63.93; H, 8.79; N, 10.29; S, 0.37; Found: C, 64.58; H, 8.05; N, 10.58; S, 0.32.

TGA and DSC were used to measure their thermal properties in bulk. All the resulting block copolymers have a high thermo-stability (T_d > 300 °C) except $N_{43}bH_{28}$ (T_d = 265.8 °C), and one glass transition temperature (T_g) in the range of 85.6 °C ~ 112.2 °C depending on their PNIPAm chain length and molecular weights. That is, the T_g shifts to lower temperature with an increase of molecular weight but higher temperature with an increase of PNIPAm block. The T_d and T_g values are listed in Table 1.

Homo-PHIPPVTA is a type of mesogen-jacketed liquid crystal polymer (MJLCP).[44,46] In order to explore the liquid-crystalline behaviors of PNIPAm-*b*-PHIPPVTA, polarized light microscope (PLM) and one-dimensional wide angle X-ray diffraction (1D WAXD) were employed. The block copolymer samples were amorphous when the molecular weight is lower than a critical molecular weight of approximately 2.76 × 10^4 g mol^{-1} for the $N_{43}bH_x$ and 4.48 × 10^4 g mol^{-1} for the $N_{151}bH_x$, respectively. The obvious birefringence of block copolymers was observed when the molecular weight is higher than the critical molecular weight (Fig.2). In addition, the birefringence remained before the decomposition temperature and the textures maintained during the cooling process. Although the birefringence of liquid crystal phase is obvious, typical liquid crystal texture is hard to be identified under PLM, and X-ray diffraction is necessary to identify the liquid crystal phase structures.

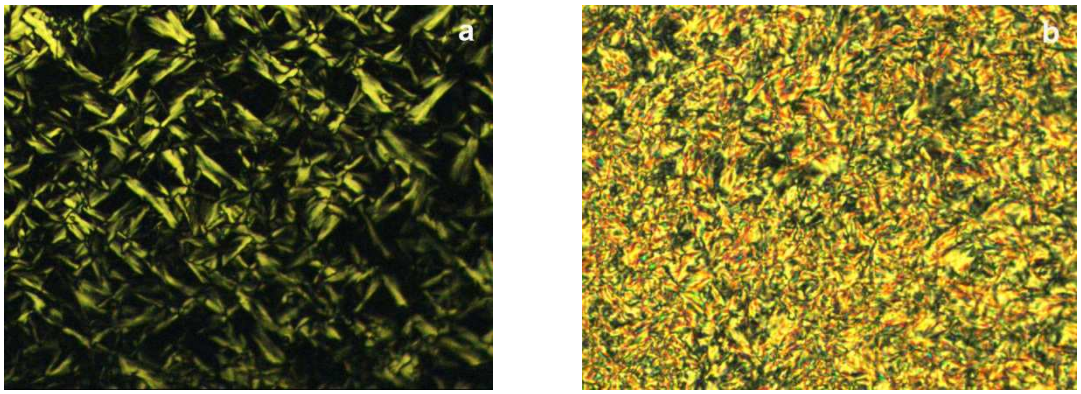

Fig.2 Representative PLM images of the textures of $N_{43}bH_{276}$ (a) and $N_{151}bH_{291}$ (b) at 140 °C.

The structural evolution of PNIPAm-*b*-PHIPPVTA during the first heating and cooling was investigated by 1D WAXD. For $N_{43}bH_x$, a sharp diffraction peak can be seen at 2θ = 5.60 ° (*d*-spacing = 1.58 nm) and 5.71° (*d*-spacing = 1.55 nm) for $N_{43}bH_{95}$ and $N_{43}bH_{276}$, respectively. And the diffraction peak of the $N_{43}bH_{95}$ and $N_{43}bH_{276}$ remain permanently after the first heating, indicating that the ordered structure of sample has been maintained, which is consistent with the PLM results. We also noted that the diffraction peak intensity decreases with decreasing temperature during the cooling process (Fig.3 and Fig.4). For instance, the intensity of $N_{43}bH_{276}$ at 30 °C is only nearly half of the one at 210 °C (Fig.4b). This indicates that the periodic electron density contrast generating this reflection reduces with decreasing temperature.[55] Compared with the diffraction peak of the $N_{43}bH_{95}$ shown in Fig.3, the diffraction peak of the $N_{43}bH_{276}$ is narrower with the intense intensity (Fig.4). In the high 2θ angle region, only an amorphous halo around 22° could be observed, indicating no long-range ordered structure formed via molecular packing.

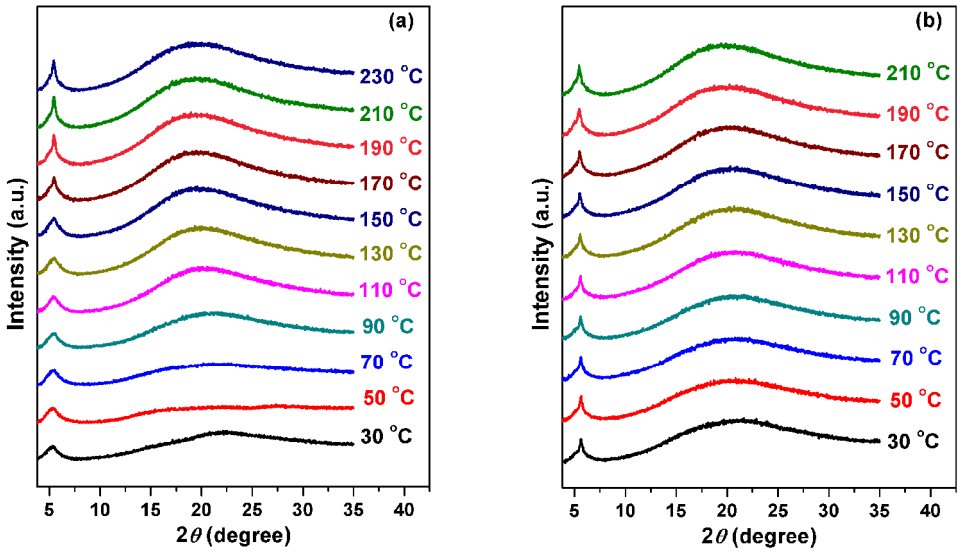

Fig.3 Sets of 1D WAXD powder patterns of $N_{43}bH_{95}$ (a) obtained during the first heating of the as-cast films. The corresponding first cooling WAXD powder patterns are shown in (b).

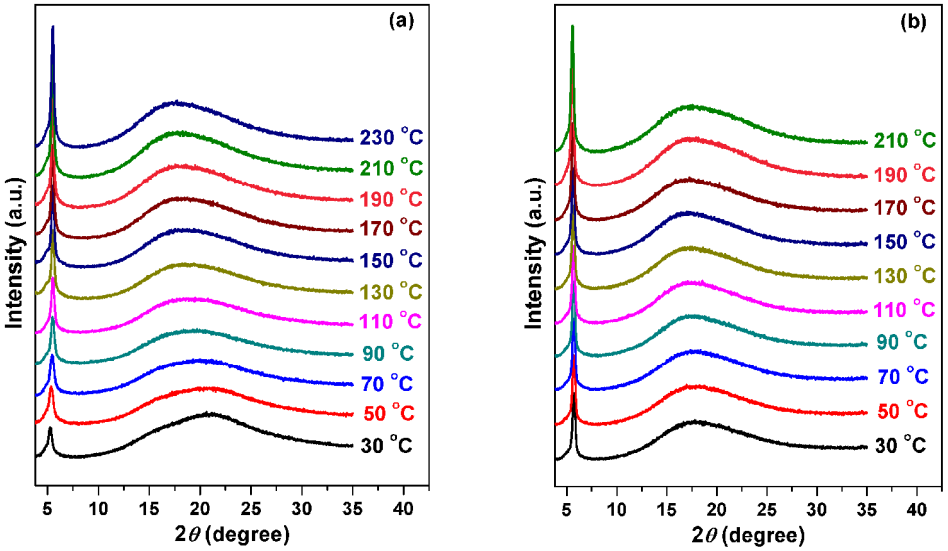

Fig.4 Sets of 1D WAXD powder patterns of $N_{43}bH_{276}$ (a) obtained during the first heating of the as-cast films. The corresponding first cooling WAXD powder patterns are shown in (b).

Sets of 1D WAXD powder patterns of $N_{151}bH_x$ are shown in Fig.5 and Fig.6. A sharp diffraction peak can be seen at 2θ = 5.54 ° (*d*-spacing = 1.60 nm) and 5.62° (*d*-spacing = 1.57 nm) for $N_{151}bH_{146}$ and $N_{151}bH_{291}$, respectively. The *d*-spacing of $N_{151}bH_x$ is same that of $N_{43}bH_x$. The ordered structures on the nanometer scale develop during the first heating. After this process, the ordered structures are permanently retained in the subsequent cooling scans. On the basis of these 1D WAXD results, it can be concluded that the length of the PNIPAm and PHIPPVTA blocks don't affect liquid crystalline behavior of the copolymers. However, the PLM and 1D WAXD patterns lack dimensionality, and 2D WAXD film patterns are necessary to identify the liquid crystal phase structures.

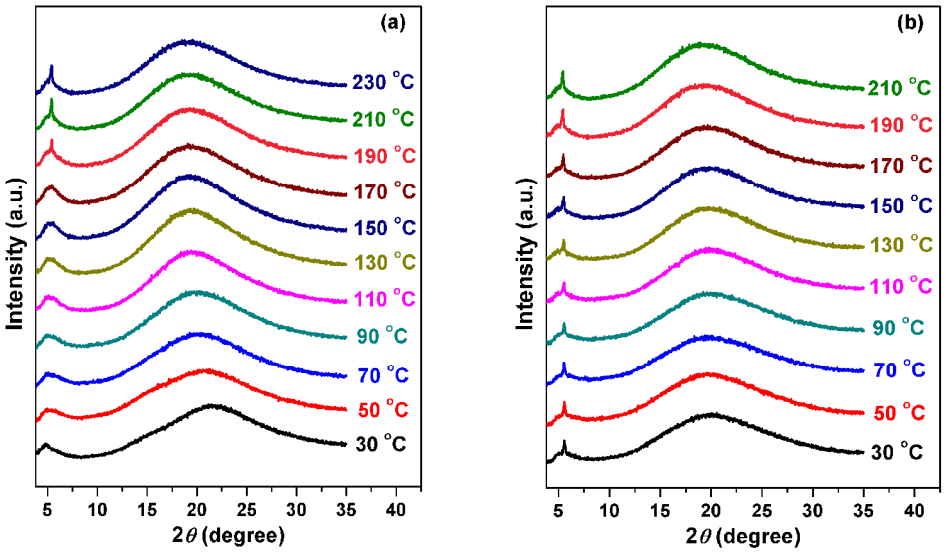

Fig.5 Sets of 1D WAXD powder patterns of $N_{151}bH_{146}$ (a) obtained during the first heating of the as-cast films. The corresponding first cooling WAXD powder patterns are shown in (b)

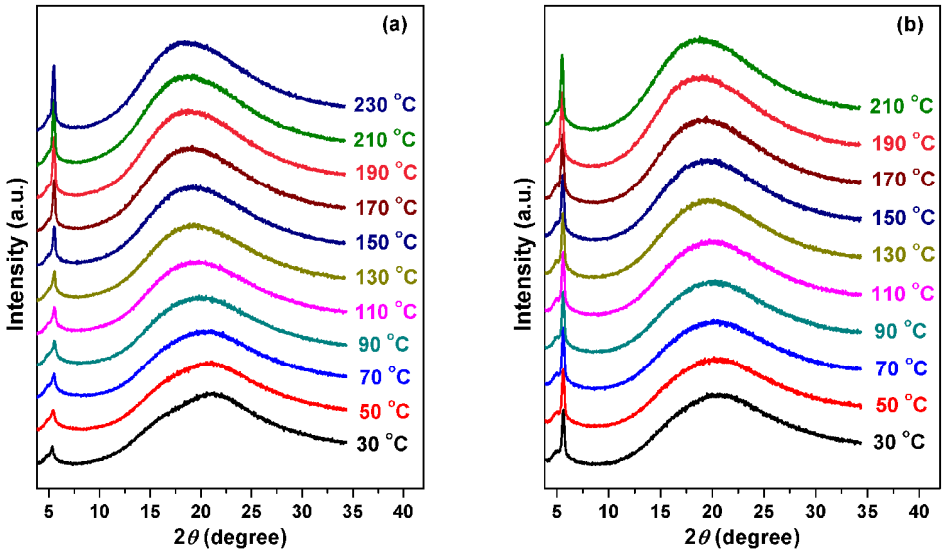

Fig.6 Sets of 1D WAXD powder patterns of $N_{151}bH_{291}$ (a) obtained during the first heating of the as-cast films. The corresponding first cooling WAXD powder patterns are shown in (b).

2D WAXD patterns of the oriented $N_{43}bH_{276}$ and $N_{151}bH_{291}$ samples are shown in Fig.7. The film samples were obtained and treated with a relatively large shear force at ~ 140 °C. The patterns were taken at room temperature with the X-ray incident beam perpendicular to the shear direction (*X* axis), and the shear gradient was along the *Z* axis. In part a and b of Fig.7, the shear direction was parallel to the meridian direction. In low 2θ angle region, only a pair of strong diffraction arcs can be seen on the equators at 2θ = 5.71° (*d*-spacing = 1.55 nm) and 5.59° (*d*-spacing = 1.58 nm) for $N_{43}bH_{276}$ and $N_{151}bH_{291}$, respectively. This suggests that the ordered structures have developed along the direction perpendicular to the shear direction on the nanometer scale. The intensity profiles along the meridian are shown in Fig.S1a, wherein the amorphous scattering maxima are located at 2θ = 20.9° (*d*-spacing = 0.43 nm) and 18.3° (*d*-spacing = 0.48 nm) for the $N_{43}bH_{276}$ and $N_{151}bH_{291}$, respectively. In addition, scattering halos in the high 2θ angle region are concentrated on the meridians with rather broad azimuthal distributions (Fig.S1b). This reveals that only the short-range orders exist along the shear direction.

Cite this: DOI: 10.1039/c0xx00000x

www.rsc.org/xxxxxx

PAPER

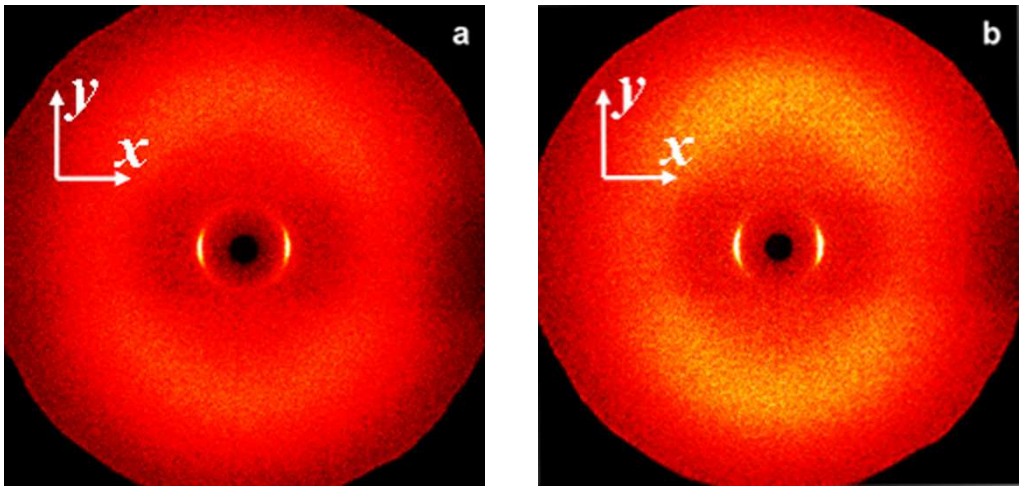

Fig.7 2D WAXD patters of $N_{43}bH_{276}$ (a) and $N_{151}bH_{291}$ (b) detected at room temperature. The X-ray incident beam is perpendicular to the shear direction (*x*).

Fig.8 presents the diffraction patterns of the $N_{43}bH_{276}$ and $N_{151}bH_{291}$with the X-ray incident beam parallel to the shear direction. In low 2θ angle region, six diffraction arcs are located at 2θ = 5.71° (*d*-spacing = 1.55 nm) and 5.59° (*d*-spacing = 1.58 nm) the $N_{43}bH_{276}$ and $N_{151}bH_{291}$, respectively. This suggests a hexagonal lateral packing of the cylinders with each cylinder having an average diameter of 1.78 nm and 1.82 nm for the $N_{43}bH_{276}$ and $N_{151}bH_{291}$, respectively. Fig.S2a and b show six maxima with an angle of 60° between the two adjacent diffraction maxima, but the azimuthal intensities are not exactly identical. This may be caused by imperfection in the sample orientation during the experiment. Nevertheless, the higher order diffractions has not been detected in Fig.S2a and Fig.S2b, indicating the hexagonal lateral packing lacks long-range order perpendicular to the shear direction. Combining 1-D and 2-D WAXD results with POM and DSC observations, it can be concluded that the ordered structure of $N_{43}bH_{276}$ and $N_{151}bH_{291}$ is a hexatic columnar nematic phase. Moreover, the length of PHIPPVTA pendant group is calculated to be approximately 2.05 nm. On the basis of these low-angle WAXD results and calculated value (2.05 nm), it can be concluded that the pendant group in the side chains tilt approximately 60° and 63° away from the cylinder long axis for the $N_{43}bH_{276}$ and $N_{151}bH_{291}$, respectively.

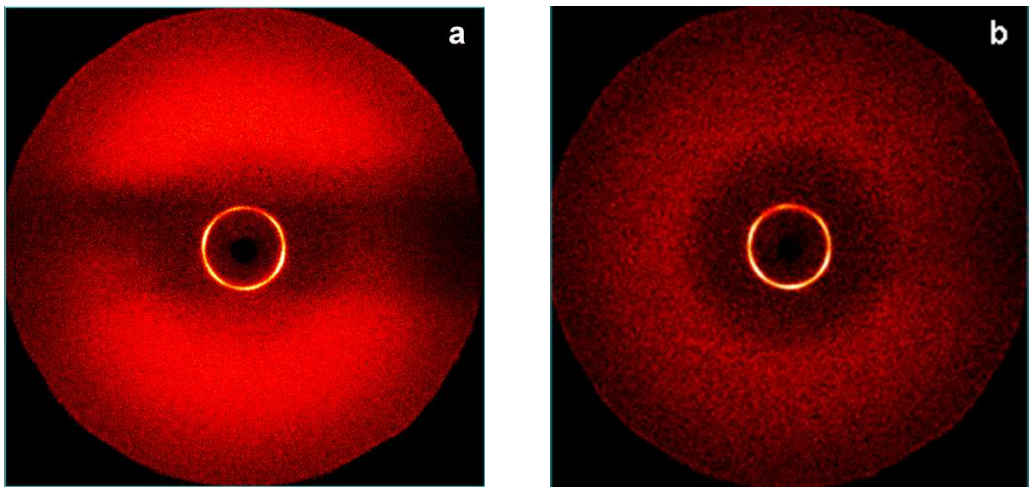

Fig.8 2D WAXD patters of $N_{43}bH_{276}$ (a) and $N_{151}bH_{291}$ (b) obtained at room temperature. The X-ray incident beam is parallel to the shear direction.

Cite this: DOI: 10.1039/c0xx00000x

www.rsc.org/xxxxxx

PAPER

Solution Property of the Block Copolymer PNIPAm-*b*-PHIPPVTA

PHIPPVTA separate from aqueous solution as the temperature exceeded cloud point due to the configuration transformation from hydrophilic soluble chains to hydrophobic collapsed domains.[44,46] Incorporation of more hydrophobic (lowering the LCST) comonomers (NIPAm) into homopolymer chains with unusual thermo-responsive properties resulted in the cloud point changes.[45] Herein, the rod-coil diblock copolymers with PHIPPVTA rod units and flexible PNIPAm coil were precisely controlled to clarify the influence of chain length and polymer composition on the thermo-responsive behavior. To obtain an obvious aggregation behavior of the PNIPAm-*b*-PHIPPVTA diblock polymer in aqueous solution, the solution concentrations for turbidity measurement are set as high as 10.0 mg ml^{-1}. The percent transmittance was subsequently monitored as a function of increasing temperature, and where a clear change in the transmittance was observed the cloud point was taken as the temperature at which the transmittance dropped to 50%. Fig.9 shows the thermo-responsive behaviors of the PNIPAm-*b*-PHIPPVTA aqueous solutions. PNIPAm-*b*-PHIPPVTAs ($N_{43}bH_x$ and $N_{151}bH_x$) are highly soluble in water at the temperature below cloud point (the transmittance of the solutions keeps constant at 100%) and start to aggregate (became opaque) at cloud point, which leads to a significant transition in the transmittance. The corresponding cooling curve in Fig.9a, almost exactly, the heating curve, and the PNIPAm-*b*-PHIPPVTA block polymer redissolves giving an optically transparent solution. By contraries, $N_{151}bH_x$ does exhibit obvious hysteresis upon cooling (Fig.9b). This is consistent with the previous reports.[56,57]

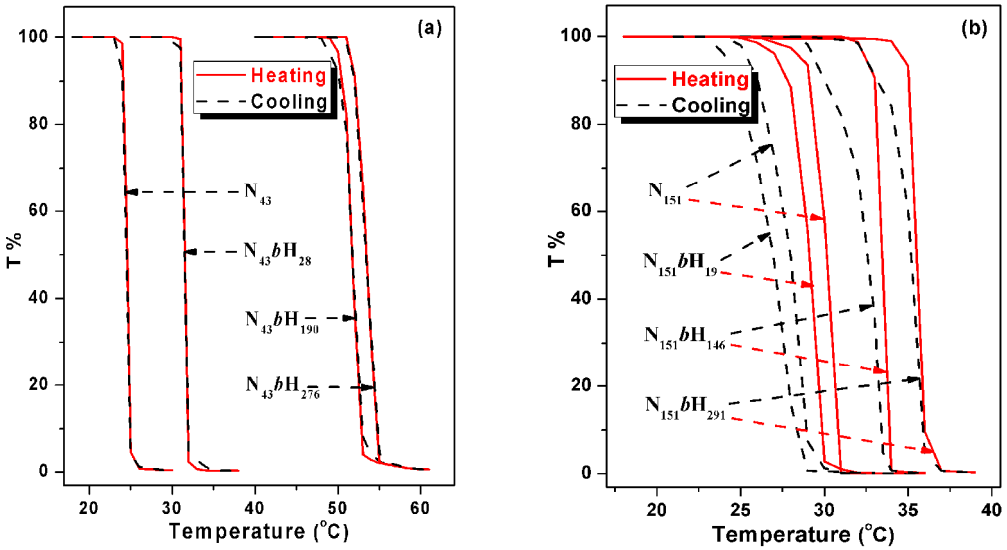

Fig.9 Heating and cooling turbidity curves for $N_{43}bH_x$ (a) and $N_{151}bH_x$ (b) block polymers at a concentration of 10.0 mg ml^{-1}.

The thermal-smart stability of aqueous $N_{43}bH_{276}$ (a) and $N_{151}bH_{291}$ (b) block copolymers solution was investigated as shown in Fig.10. The experimental results demonstrated excellent reversibility for several cycles and a quick transition between aggregation and redissolution. The reversibility in solution was stable. This reversibility was also exists at other PNIPAm-*b*-PHIPPVTA solution. A similar stability of thermo-responsive behaviour has been observed in other thermo-responsive copolymers [e.g., poly(2-(dimethylamino)ethyl methacrylate)-*b*-poly(acrylic acid) and poly(2-isopropoxy-2-oxo-1,3,2-dioxaphospholane-*co*-2-Ethoxy-2-oxo-1,3,2-dioxaphospholane)].[58,59]

Cite this: DOI: 10.1039/c0xx00000x

www.rsc.org/xxxxxx

PAPER

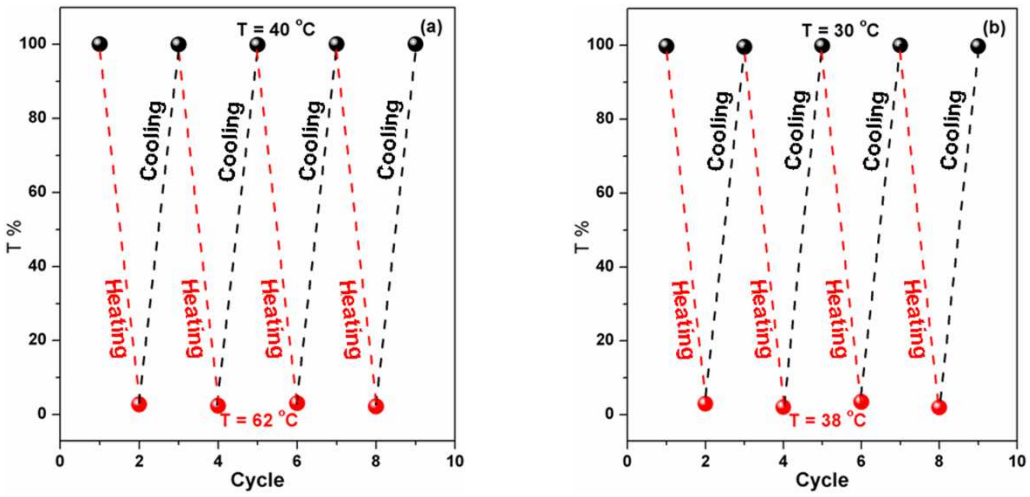

Fig.10 Reversibility of 10.0 mg ml^{-1} $N_{43}bH_{276}$ (a) and $N_{151}bH_{291}$ (b) solutions at two different temperatures.

The relationship between cloud point and degree of polymerization (DP) of PHIPPVTA block was studied as shown in Fig.11. In the $N_{43}bH_x$ samples, the cloud point of solution rapidly increased by 27.2 °C when the DP of PHIPPVTA increased from 0 to 190, while the increase of cloud point is smaller in the higher DP (> 190). Namely, the cloud point increases linearly with the DP of PHIPPVTA block (190 > DP > 0). The similar dependence of cloud point on the DP has been observed in other thermo-responsive polymers.[60] However, the cloud points of the $N_{151}bH_x$ on DP dependence aren't significant compared with that of the $N_{43}bH_x$. For instance, the cloud point of $N_{151}bH_x$ solution increased by just 5.3 ℃ when it's DP of PHIPPVTA block changed from 0 to 291. This suggesting that the cloud point of block copolymer with smaller DP of flexible chain PNIPAm block depend more on DP of the semi-rigid PHIPPVTA block. Contrarily, the cloud point of block copolymer with higher DP of flexible chain PNIPAm block is less affected by the DP of the semi-rigid PHIPPVTA block. This trend may be attributed to the hydrophilic-hydrophobic effect. While the mechanism of this significant cloud point dependency is not clear, we believe it is probably attributes to the chain rigidity.

The cloud point of PHIPPVTA remarkably increased with increasing of its molecular weight. Namely, the hydrophobicity of PHIPPVTA decreased with increasing of its molecular weight. For instance, the cloud point of HIPPVTA was 24 °C and 80.9 °C at molecular weight of 0.47 × 10^4 g mol^{-1} and 4.42 × 10^4 g mol^{-1}, respectively.[44] Therefore, the cloud point of $N_{151}bH_{19}$ is lower than that of N_{151}, and the cloud point of PNIPAm-*b*-PHIPPVTAs increased with increasing of PHIPPVTA block DP. These observations imply that the cloud points of rod-coil diblock copolymers in water were determined by both blocks. A further investigation is underway.

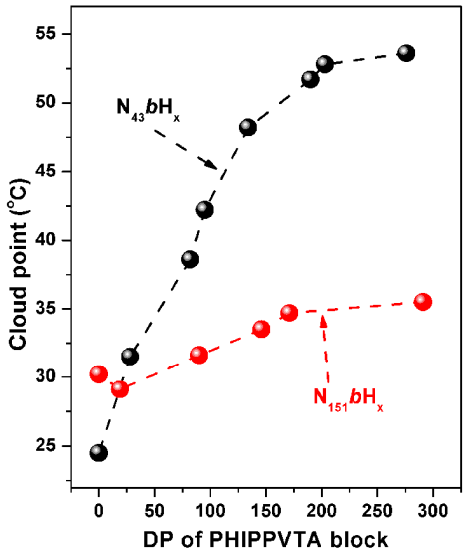

Fig.11 Cloud point of $N_{43}bH_x$ and $N_{151}bH_x$ as a function of x (x indicates the DP of PHIPPVTA block)

We also noted that the decreasing rate of the cloud point varied in different copolymer concentration regions. The results are summarized in Fig.12. The cloud point decreased exponentially other than linearly with the increasing of polymer concentration. Namely, the cloud point decreased more obvious in a dilute concentration range. For example, the cloud point of $N_{43}bH_{276}$ decreased by 25.9 °C when its concentration changed from 1 to 5 mg ml^{-1} while its cloud point decreased by 1.5 °C when the concentration changes from 15 to 20 mg ml^{-1}. The similar dependence of cloud point on the block copolymer concentration has been observed in $N_{151}bH_x$. For instance, the cloud point of $N_{151}bH_{291}$ decreased by 8.0 °C when its concentration changed from 1 to 5 mg ml^{-1} while its cloud point

decreased by 1.2 °C when the concentration changes from 15 to 20 mg ml^{-1}. The similar dependence of the cloud points on the concentration has been observed in other thermo-responsive polymers. [61-63]

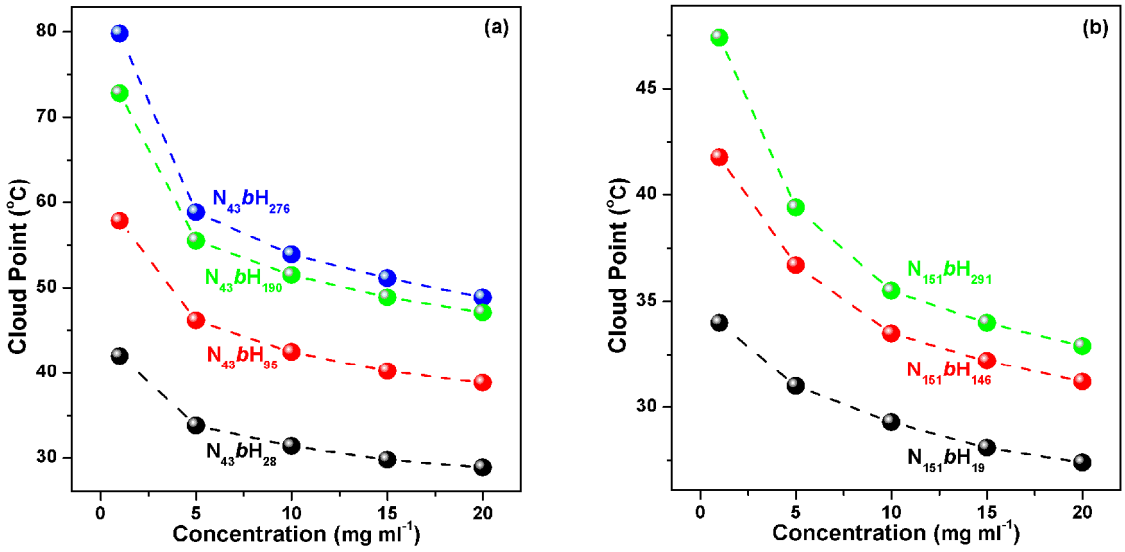

Fig.12 Cloud point of $N_{43}bH_x$ (a) and $N_{151}bH_x$ (b) block polymers solution as a function of concentration

Conclusions

We successfully synthesized a well-defined thermo-sensitive rod-coil diblock copolymer PNIPAm-*b*-PHIPPVTA consisting of poly[bis(*N*-hydroxyisopropyl pyrrolidone) 2-vinylterephthalate] (PHIPPVTA) rod units as a semirigid segment and flexible chains such as PNIPAm by RAFT polymerization. The molecular weights of the diblock copolymers were confirmed by GPC and ^{1}H NMR. Liquid-crystalline behaviors of these diblock copolymers were investigated through a combined approach of DSC, PLM, 1D WAXD and 2D WAXD. The results showed that hexatic columnar nematic phase were demonstrated when $N_{43}bH_x$ and $N_{151}bH_x$ with X $\geq$ 95 and 146, respectively. Turbidity measurement results revealed the cloud point of diblock copolymers exhibited remarkable molecular weight-dependence and concentration-dependence. That is, the cloud point of diblock copolymers decreased with decreasing of PHIPPVTA block DP. The cloud point of diblock copolymers decreased with increasing of copolymer solution concentration. What's more, the more significant molecular weight-dependence and concentration-dependence on cloud point have been observed in $N_{43}bH_x$ solution than in $N_{151}bH_x$ solution.

Acknowledgments

This work was supported by the Innovation Platform Open Fund Projects of University of Hunan Province (10k067), the postgraduate research and innovation project of Hunan province (CX2012A010) and the National Nature Science Foundation of China (51073131).

References:

[1]Coelho J., Ferreira P., Alves P., Cordeiro R., Fonseca A., Góis J. and Gil M. *The EPMA Journal* **2010**, *1*, 164-209.
[2]Mecke A., Dittrich C. and Meier W. *Soft Matter* **2006**, *2*, 751-759.
[3]Madsen J., Armes S. P., Bertal K., Lomas H., MacNeil S. and Lewis A. L. *Biomacromolecules* **2008**, *9*, 2265-2275.
[4]Chassenieux C., Nicolai T. and Benyahia L. *Current Opinion in Colloid & Interface Science* **2011**, *16*, 18-26.
[5]Tsitsilianis C. *Soft Matter* **2010**, *6*, 2372-2388.
[6]He C., Kim S. W. and Lee D. S. *Journal of Controlled Release* **2008**, *127*, 189-207.
[7]Alexander C. and Shakesheff K. M. *Advanced Materials* **2006**, *18*, 3321-3328.
[8]Mano J. F. *Advanced Engineering Materials* **2008**, *10*, 515-527.
[9]Jiang X. and Zhao B. *Macromolecules* **2008**, *41*, 9366-9375.
[10]Jiang X., Lavender C. A., Woodcock J. W. and Zhao B. *Macromolecules* **2008**, *41*, 2632-2643.
[11]Jiang J., Tong X., Morris D. and Zhao Y. *Macromolecules* **2006**, *39*, 4633-4640.
[12]Shinke Y., Kanazawa A., Kanaoka S. and Aoshima S. *Journal of Polymer Science Part A: Polymer Chemistry* **2013**, *51*, 5239-5247.
[13]Liu F., Seuring J. and Agarwal S. *Journal of Polymer Science Part A: Polymer Chemistry* **2012**, *50*, 4920-4928.
[14]Tang S., Cao Y., Goddard S. C. and He W. *Journal of Polymer Science Part A: Polymer Chemistry* **2014**, *52*, 112-120.
[15]Han X., Zhang X., Zhu H., Yin Q., Liu H. and Hu Y. *Langmuir* **2013**, *29*, 1024-1034.
[16]Schmaljohann D. *Advanced Drug Delivery Reviews* **2006**, *58*, 1655-1670.
[17]Liu X. M., Wang L. S., Wang L., Huang J. and He C. *Biomaterials* **2004**, *25*, 5659-5666.
[18]Jochum F. D. and Theato P. *Chemical Communications* **2010**, *46*, 6717-6719.
[19]Wu C. and Zhou S. *Macromolecules* **1995**, *28*, 8381-8387.
[20]Wu C. and Zhou S. *Macromolecules* **1995**, *28*, 5388-5390.
[21]Hu L., Sarker A. K., Islam M. R., Li X., Lu Z. and Serpe M. J. *Journal of Polymer Science Part A: Polymer Chemistry* **2013**, *51*, 3004-3020.
[22]Xiong Z., Peng B., Han X., Peng C., Liu H. and Hu Y. *Journal of Colloid and Interface Science* **2011**, *356*, 557-565.
[23]Yan J., Ji W., Chen E., Li Z. and Liang D. *Macromolecules* **2008**, *41*, 4908-4913.
[24]Liu X., Luo S., Ye J. and Wu C. *Macromolecules* **2012**, *45*, 4830-4838.
[25]Zhao J., Zhang G. and Pispas S. *The Journal of Physical Chemistry B* **2009**, *113*, 10600-10606.
[26]Nuopponen M., Ojala J. and Tenhu H. *Polymer* **2004**, *45*, 3643-3650.
[27]Adelsberger J., Kulkarni A., Jain A., Wang W., Bivigou-Koumba A. M., Busch P., Pipich V., Holderer O., Hellweg T., Laschewsky A.,

Müller-Buschbaum P. and Papadakis C. M. *Macromolecules* **2010**, *43*, 2490-2501.
[28] Arotçaréna M., Heise B., Ishaya S. and Laschewsky A. *Journal of the American Chemical Society* **2002**, *124*, 3787-3793.
[29] Jin N., Zhang H., Jin S., Dadmun M. D. and Zhao B. *Macromolecules* **2012**, *45*, 4790-4800.
[30] Weiss J. and Laschewsky A. *Macromolecules* **2012**, *45*, 4158-4165.
[31] Hu Y., Darcos V., Monge S. and Li S. *Journal of Polymer Science Part A: Polymer Chemistry* **2013**, *51*, 3274-3283.
[32] Matsuyama T., Shiga H., Asoh T.-A. and Kikuchi A. *Langmuir* **2013**, *29*, 15770-15777.
[33] Shi X.-J., Chen G.-J., Wang Y.-W., Yuan L., Zhang Q., Haddleton D. M. and Chen H. *Langmuir* **2013**, *29*, 14188-14195.
[34] Vo C.-D., Rosselgong J., Armes S. P. and Tirelli N. *Journal of Polymer Science Part A: Polymer Chemistry* **2010**, *48*, 2032-2043.
[35] Minoda M., Shimizu T., Miki S. and Motoyanagi J. *Journal of Polymer Science Part A: Polymer Chemistry* **2013**, *51*, 786-792.
[36] Miasnikova A. and Laschewsky A. *Journal of Polymer Science Part A: Polymer Chemistry* **2012**, *50*, 3313-3323.
[37] Bi Y., Yan C., Shao L., Wang Y., Ma Y. and Tang G. *Journal of Polymer Science Part A: Polymer Chemistry* **2013**, *51*, 3240-3250.
[38] Patil N., Roy S. G., Haldar U. and De P. *The Journal of Physical Chemistry B* **2013**, *117*, 16292-16302.
[39] Otsuka I., Fuchise K., Halila S., Fort S. b., Aissou K., Pignot-Paintrand I., Chen Y., Narumi A., Kakuchi T. and Borsali R. *Langmuir* **2009**, *26*, 2325-2332.
[40] Kim H.-J., Kim T. and Lee M. *Accounts of Chemical Research* **2010**, *44*, 72-82.
[41] Huang C.-J. and Chang F.-C. *Macromolecules* **2008**, *41*, 7041-7052.
[42] Rao J., Luo Z., Ge Z., Liu H. and Liu S. *Biomacromolecules* **2007**, *8*, 3871-3878.
[43] Wang C., Du F., Xie H., Zhang H., Chen E. and Zhou Q. *Chemical Communications* **2010**, *46*, 3155-3157.
[44] Liu P., Xie H., Tang H., Zhong G. and Zhang H. *Journal of Polymer Science Part A: Polymer Chemistry* **2012**, *50*, 3664-3673.
[45] Liu P., Tang W. and Zhang H. *Polymer* **2013**, *54*, 4902-4908.
[46] Liu P., Tan Q., Xiang L. and Zhang H. *Journal of Polymer Science Part A: Polymer Chemistry* **2013**, *51*, 3429-3438.
[47] Mitsukami Y., Donovan M. S., Lowe A. B. and McCormick C. L. *Macromolecules* **2001**, *34*, 2248-2256.
[48] Zhang D., Liu Y., Wan X. and Zhou Q. F. *Macromolecules* **1999**, *32*, 4494-4496.
[49] Convertine A. J., Lokitz B. S., Vasileva Y., Myrick L. J., Scales C. W., Lowe A. B. and McCormick C. L. *Macromolecules* **2006**, *39*, 1724-1730.
[50] Xu J. and Liu S. *Soft Matter* **2008**, *4*, 1745-1749.
[51] Zhou C., Hillmyer M. A. and Lodge T. P. *Macromolecules* **2011**, *44*, 1635-1641.
[52] Wen G.-H., Zhang B., Xie H.-L., Liu X., Zhong G.-Q., Zhang H.-L. and Chen E.-Q. *Macromolecules* **2013**, *46*, 5249-5259.
[53] Liou G.-S., Hsiao S.-H., Ishida M., Kakimoto M. and Imai Y. *Journal of Polymer Science Part A: Polymer Chemistry* **2002**, *40*, 3815-3822.
[54] Yang C.-P., Chen R.-S. and Chen J.-A. *Journal of Polymer Science Part A: Polymer Chemistry* **2000**, *38*, 1-8.
[55] Ye C., Zhang H.-L., Huang Y., Chen E.-Q., Lu Y., Shen D., Wan X.-H., Shen Z., Cheng S. Z. D. and Zhou Q.-F. *Macromolecules* **2004**, *37*, 7188-7196.
[56] Cheng H., Shen L. and Wu C. *Macromolecules* **2006**, *39*, 2325-2329.
[57] Keerl M., Smirnovas V., Winter R. and Richtering W. *Angewandte Chemie International Edition* **2008**, *47*, 338-341.
[58] Xiong Z., Peng B., Han X., Peng C., Liu H. and Hu Y. *J Colloid Interface Sci* **2011**, *356*, 557-565.
[59] Iwasaki Y., Wachiralarpphaithoon C. and Akiyoshi K. *Macromolecules* **2007**, *40*, 8136-8138.
[60] Roeser J., Moingeon F., Heinrich B., Masson P., Arnaud-Neu F., Rawiso M. and Méry S. *Macromolecules* **2011**, *44*, 8925-8935.
[61] Jiang X. and Zhao B. *Journal of Polymer Science Part A: Polymer Chemistry* **2007**, *45*, 3707-3721.
[62] Shimomoto H., Kanaoka S. and Aoshima S. *Journal of Polymer Science Part A: Polymer Chemistry* **2012**, *50*, 4137-4144.
[63] Tong Z., Zeng F., Zheng X. and Sato T. *Macromolecules* **1999**, *32*, 4488-4490.